5. A STRUT WITH INFINITELY ADJUSTABLE THERMAL EXPANSIVITY AND LENGTH

By Paul T. Nelson

TRW Systems Group

SUMMARY

TRW Systems has developed a tubular strut with an integral mechanism for adjusting its thermal expansivity and length. The stimulus for its development derived from the stringent thermal stability requirements anticipated for the metering truss in the Large Space Telescope (LST). Its application is not limited to the LST or even to spacecraft structures; its features may be advantageously applied to a general variety of structures and precision mechanisms where dimensional control of component elements in a dynamic thermal environment is required. Detail design, fabrication, and test of a developmental strut have been completed.

INTRODUCTION

A significant and ever increasing category of spacecraft structures has to be substantially inert to the dynamic thermal environment on orbit. The metering structure for the Large Space Telescope (LST) falls in this category. Since it is a precision optical structure, its allowable distortion due to temperature changes is near zero. A prime candidate for the metering structure is a cylindrical truss consisting of several circumferential rings interconnected by tubular strut members. Figure 1 illustrates this concept and shows how a temperature gradient change along the axis can cause dimensional changes in the rings and the struts. However, if the expansivity relationship of ring to strut is properly proportioned, as shown in the inset, the truss length will nominally remain constant. This is because the ring expansion is proportioned to compensate for strut expansion and is called athermalization. A severe constraint results on control of the expansivities (α_R, α_S) of the rings and struts, however.

A straightforward means of controlling the required ratio of α_R/α_S is to fabricate the circular rings to an acceptable expansivity range and then adjust, to suit, the expansivity of their interfacing struts. Strut expansivity can be precisely adjusted by the simple tuning principle described in this paper.

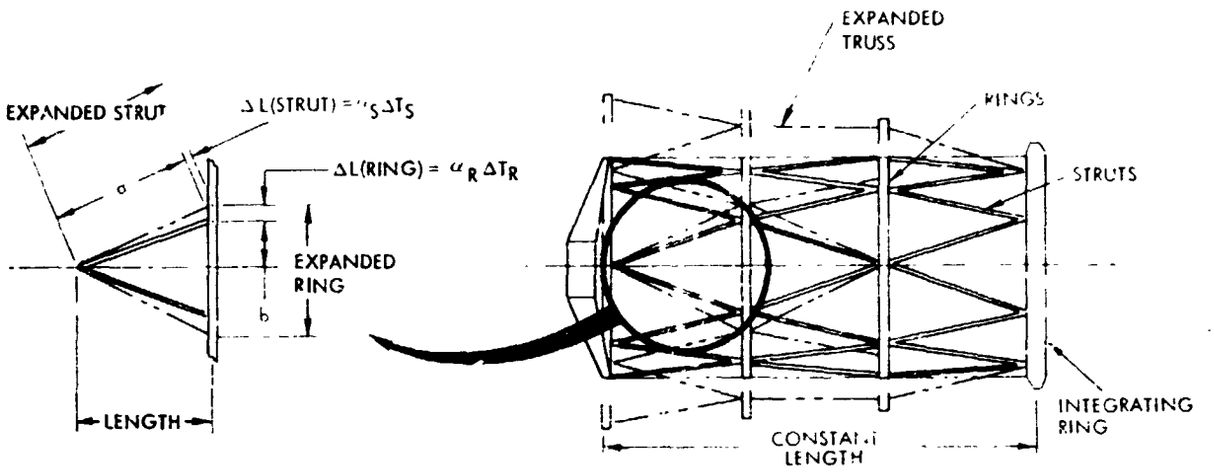

Figure 1. - Effect of temperature gradient change on an athermalized truss.

Graphite/epoxy is a prime material candidate for the LST metering truss. It is uniquely suited for this application because of its low coefficient of thermal expansion (CTE), high thermal conductivity, low specific heat, high specific stiffness, and high specific strength. Even with these outstanding material properties, when used in the LST metering truss and enclosed in multilayer insulation, tests indicate that variations in its CTE are intolerable. In fact, conventional design approaches using any common construc.tional materials available today, even with the most sophisticated fabricatio.. methods, are expected to be inadequate for the critical structure in the LST because of its stringent thermal stability requirements. The expansivity tolerance band—due to variations in constituent materials and processing—cannot be held small enough.

Figure 2. - Graphite/epoxy athermal strut with tunable end fittings.

Figure 2 shows a developmental structural member that is representative of a strut for a three-bay metering truss of LST size. The tubular portion of the strut is made of graphite epoxy with longitudinal graphite fiber orientation and Style 181 glass cloth on inside and outside dia- -trical surfaces. This construct. . yields a relatively low positive CTE, but, because of variations in materials and processing, it does not yield adequate repeatability i- -roduction for athermalization wi'' a means for "tuning." The end f .gs are metallic, nonferromagnetic, and incorporate a mechanism which provides adjustment capability to "fine tune" both the pin-to-pin length and "Effective CTE" of the strut. It is this

adjustment feature that compensates for the inadequacy of conventional structural design practice for athermal structures and is the main topic of this paper.

SYMBOLS

L	length
ΔL	change in length due to temperature change
ΔT	change in temperature
α	coefficient of thermal expansion

Subscripts:

Al	aluminum
eff	effective
G	graphite/epoxy
R	ring
S	strut
Ti	titanium
tot	total

ATHERMAL STRUT MECHANISM

The key to achieving precision control of thermal expansivity in the strut is the mechanism illustrated in Figure 3. The primary load path for a typical tension or compression load is from the graphite-epoxy tube through the bonded titanium collar, into the threaded aluminum sleeve, and finally through the titanium eyebolt. The sleeve and eyebolt locknuts serve to retain the adjustment after it has been made and also to eliminate backlash in the mechanism. The eyebolt locknut also serves as a linear bearing for the eyebolt.

To visualize the operating principle of the mechanism, consider a uniform temperature rise in the entire system. We are primarily interested in the axial change in length induced by a change in temperature (ΔT). In this particular system, the coefficient of thermal expansion of each component will expand in direct proportion to its CTE and effective length, and thereby each component influences the overall length of the strut. The key to controlling the thermal expansivity of the strut system is the relatively high reverse

expansion of the aluminum sleeve which compensates for the aggregate positive expansion of all the other components. The strut also has infinitely variable length adjustment within the limits of thread length. This is achieved by left-hand threads on one end of the complete strut and right-hand threads on the other; thus the strut length can be fine tuned in turnbuckle fashion and locked in place with the two jam nuts.

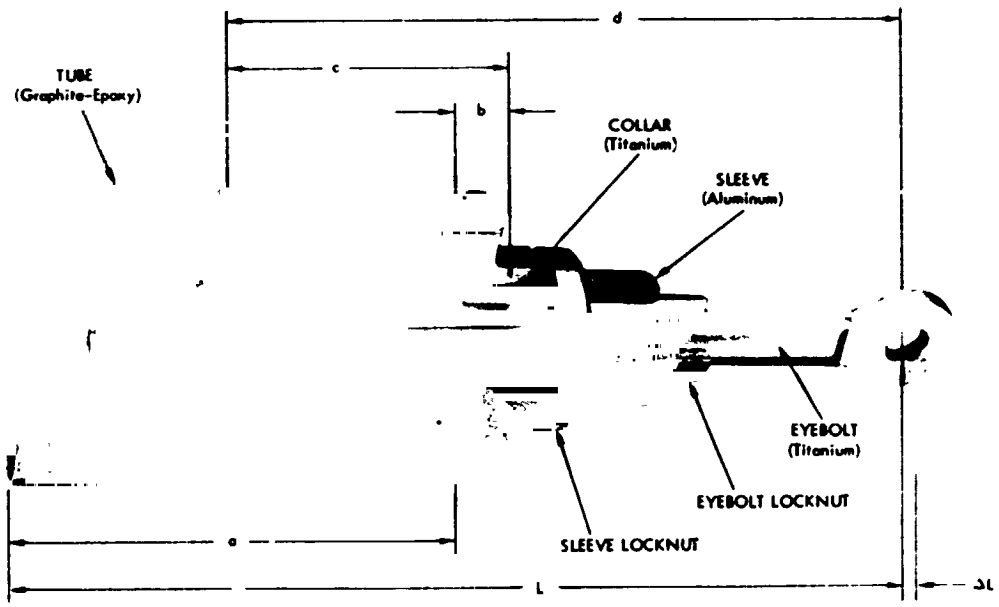

Figure 3. - View of sectional tunable end fitting.

If the procedure is followed of first adjusting the length to a nominal dimension and then adjusting thermal expansion, a further fine length adjustment will have a trivial effect on the calibrated expansivity of the strut system.

You will note that the change in length (ΔL) of the system represented in Figure 3 due to a uniform ΔT is the aggregate response of the components in the load path. In the concept reported here, the expansion of all components except the aluminum sleeve tends to increase the length of the strut. The precise increase in length (ΔL) of the complete strut system, the aggregate response of the system, is as follows:

$$\Delta L = (a\alpha_G + b\alpha_{Ti} - c\alpha_{Al} + d\alpha_{Ti})\,\Delta T_S$$

The effective CTE of the system (as shown in Figure 3) is expressed by the following:

$$\alpha_{eff} = \frac{a\alpha_G + b\alpha_{Ti} - c\alpha_{Al} + d\alpha_{Ti}}{L}$$

From the above equation it is apparent that the effective expansivity of a strut is a function of: (1) the geometry (dimensions a, b, c, d, and L) and (2) the coefficients of thermal expansion (α_G, α_{Ti}, and α_{Al}) of the constituent materials. The effective coefficient of thermal expansion of the system can be made equal to "zero" for a given selection of materials by using a geometry in which the numerator of the above equation equates to zero. Since the "c" dimension can be adjusted about its nominal value, the effective CTE of the strut "system" can be adjusted accordingly, limited only by the adjusting range of the threads. The overall length "L" is unaltered by the CTE adjustment (changing "c") because the thread series on the sleeve and eyebolt are identical; i. e., the thread pitches are the same.

FABRICATION

The graphite/epoxy tube is a six-ply unidirectional laminate of Modmor Type 1/5208 material. It was laid up on an aluminum alloy mandrel with a 0.30-mm taper over its length. A lamina of Style 181 glass cloth/5208 was laid up on both the inside and outside walls of the tube. The prepegged tubular laminate was vacuum bagged and cured for 3 hours at 107°C at 0.5×10^6 newton/m^2 autoclave pressure. This description is of the part that was tested and is not intended to imply a choice for the LST metering truss. The adjustable end-fitting components were made of stock aluminum and titanium alloys and were machined in a conventional manner. An extra assembly was made for sectioning (as shown in Figure 3) to more graphically illustrate the mechanism.

STRUT SYSTEM TESTS

Test Procedure

Tests performed on the strut assembly shown in Figure 2 included the full range of expansivity adjustment of both end fittings. The primary purpose of the tests was to verify the effectiveness of the thermal expansion tuning concept.

The test setup is shown on a 3.7-meter granite surface table with the test article inside a specially built thermal chamber (as illustrated in Figure 4). The operating principle of the experiment is as follows. A quartz spacer reacts externally against a heavy weight cast iron anchor at one end of the thermal chamber, and another spacer with the strut in between bears against a laser retroreflector at the opposite end. A steel coil spring maintains about 45 newtons force against the retroreflector throughout the tests assuring continuing compliance of the retroreflector with test specimen dilation. The retroreflector base is free to move with the free end of the test article and quartz spacer.

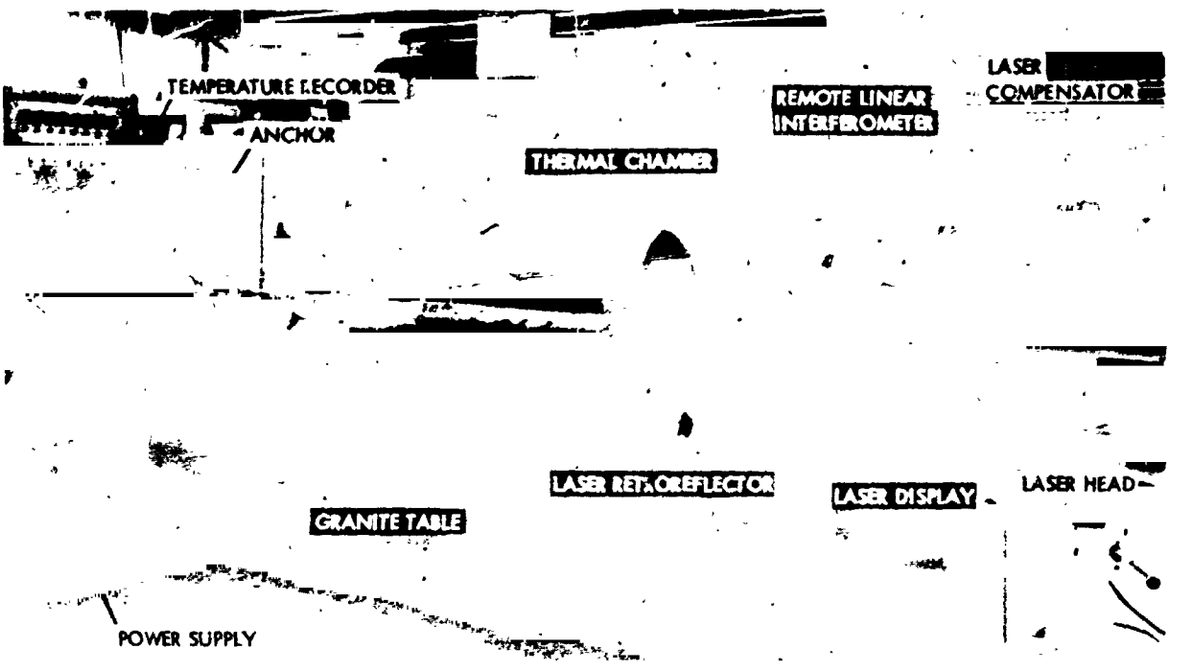

Figure 4. - Dilatometer for testing thermal expansivity of a long strut.

Figure 5. - Instrumented strut with quartz spacers at each end.

The externally positioned remote linear interferometer is the basic reference from which distance to the laser retroreflector is measured. The laser head and laser display were located in a convenient position for viewing. Figure 5 shows the instrumented strut with 15.24-cm quartz spacer rods at each end. Three thermocouples were mounted on the graphite/epoxy tube — one in the center, and one 15.24 cm from each end. A thermocouple was installed 7 cm from the outboard end of each quartz spacer. The reaction bar shown in Figure 6 assures a positive force against the anchor through the coil spring, the retroreflector, and quartz spacers, as well as the test article; it is held in place by the heavy cast iron angle plates.

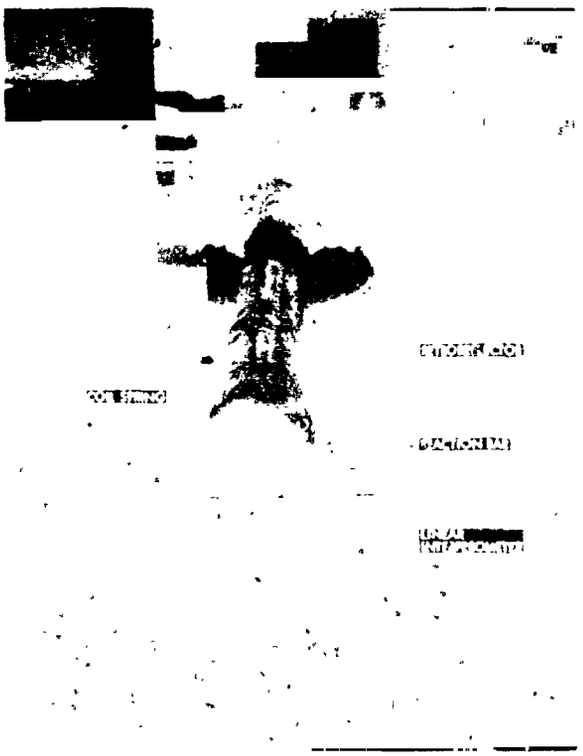

Figure 6. - View of dilatometer showing retroreflector spring reaction bar.

Figure 7 shows the laser retroreflector setup. Its polished base was well lubricated with silicon oil to assure virtually friction-free motion. The thermal chamber was heated by electrical resistance heaters and wrapped with fiberglass and aluminum foil insulation. Insulation was partially stripped in the center because of a minor temperature imbalance in the test specimen. Stripping enhanced local cooling, providing a more even temperature distribution in the tube.

Vee-shaped support clips in the chamber held the tube specimen in the center of the chamber. End caps supported the quartz spacers (as shown in Figure 8) and allowed the spacers to move freely with test specimen and spacer dilation.

The validity of this test method was verified by a preliminary experiment in which an alternate method was also evaluated. The retroreflector and remote linear interferometer in the alternate method were mounted at

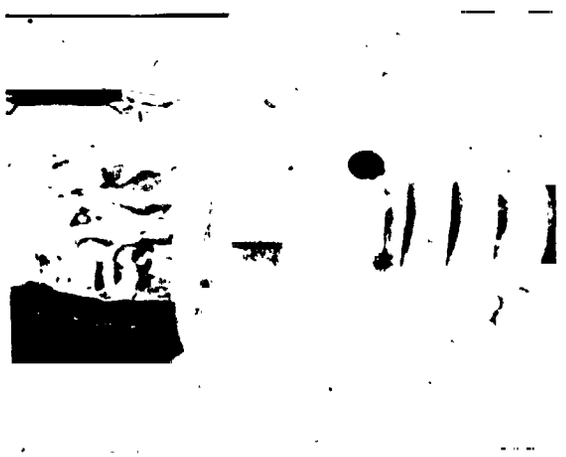

Figure 7. - Laser retroreflector setup.

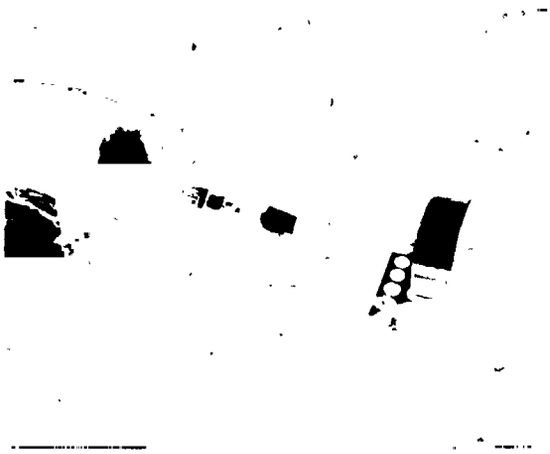

Figure 8. - End caps removed from chamber to show support of quartz spacers.

opposite ends of the test specimen which was not anchored at one end. Atmospheric turbulence in the environment surrounding the specimen, however, caused an unacceptable wavering in the laser display readout. On the other hand, an experiment directed toward a test as finally executed resulted in a very stable readout (within ±0. 025 micron), when the granite table was locally heated in the most critical area beyond tolerance to human touch. During this latter experiment, an aluminum tube was installed for protection of the laser beam to preclude atmospheric disturbance. When it was ascertained that any error due to table heating was negligible, the concept of an anchor at one end and movable retroreflector was verified. The linear interferometer could then be located close to the retroreflector (as shown in Figure 6) without the need for a protective tube for the laser beam. This latter approach appeared to be better and was accordingly selected. The experiment also confirmed that the effect of air turbulence to the laser beam over a short distance was negligible.

The strut assembly was installed in the test chamber with the quartz spacers and instrumentation. Thermocouples were installed on the graphite/epoxy tube (three places), on both end fittings, and on the quartz spacers. The length of the strut was adjusted by turning the eyebolts so that the distance between the quartz spacers (overall length) was 198 cm. This 198-cm length was nominally maintained for all of the tests. Each test run was started with the specimen relatively near room temperature. Temperature recordings were made for each thermocouple location and the laser display was reset to zero. With this pretest activity complete, the chamber was heated to a peak temperature and then allowed to level out and cool until all test specimen thermocouples and also quartz spacer thermocouples were stabilized. Temperatures were again recorded for end-of-run condition.

Test Results

Three end-fitting adjustment positions were tested: (1) sleeve full in; (2) sleeve at mid-position; and (3) sleeve full out. These positions correspond to minimum, median, and maximum effective CTE adjustments, respectively. The average temperature of the strut and quartz spacers at the beginning and end of the run are listed in Table 1. Temperature data and the corresponding change in length (ΔL) were taken when all thermocouples on the strut were within 2. 8°C. Furthermore, both quartz spacers were within 2. 8°C.

The average temperature differences (ΔT's) for the strut and spacers are also shown in Table 1. The effective strut coefficient of thermal expansion (α_S) is shown in the extreme right column. It is computed from the following:

$$\alpha_S = \frac{\Delta L_{tot} - 2L_Q \Delta T_Q \alpha_Q}{L_S \Delta T_S}$$

In this case the length of each spacer (L_Q) is 15. 24 cm and overall length of the strut (L_S) is 198 cm.

Table 1. - Temperature and expansion data from strut system test.

Test Configuration	Average Temperature at Start of Test (°C)		Average Temperature at End of Test (°C)		ΔT_Q (°C)	ΔT_S (°C)	ΔT_{tot} (cm x 10^{-4}	α_S (ppm/°C)
	Quartz Spacer	Strut System	Quartz Spacer	Strut System				
Aluminum sleeve turned in line with flats	23.1	23.1	63.6	66.0	40.4	42.9	15.4	0.10
Aluminum sleeve at mid-position	22.8	22.8	83.8	86.6	61.0	63.8	59.0	0.39
Aluminum sleeve turned to maximum outward position	21.9	22.8	80.6	83.4	58.7	60.7	93.0	0.69

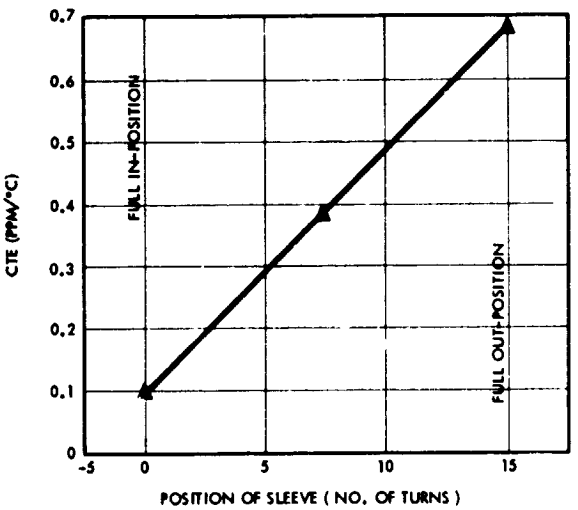

Figure 9. - Effective CTE versus position of aluminum sleeve.

A total number of 15 turns comprised the full range of adjustment. Therefore, the sensitivity of adjustment is as follows:

$$\frac{0.69 - 0.10}{15} = 0.039 \text{ ppm/°C/turn}$$

Linearity of the adjustment is shown by the curve in Figure 9.

CONCLUDING REMARKS

The strut was "tuned" from 0.10 to 0.69 ppm/°C. Adjustment of expansivity is substantially linear in the adjustment range. A much wider range of expansion could be readily demonstrated by appropriate material and geometry selection. Clearly the adjustment range could be made to pass through zero and into negative values. Viability of this TRW tuning concept is proven and can be applied "in-principle" to a wide range of thermally inert structural or mechanical systems.